

# THINGSvision: a Python toolbox for streamlining the extraction of activations from deep neural networks

Lukas Muttenthaler, Martin N. Hebart

Vision and Computational Cognition Group,

Max Planck Institute for Human Cognitive and Brain Sciences, Leipzig, Germany

Corresponding authors: Lukas, L.M., Muttenthaler; [muttenthaler@cbs.mpg.de](mailto:muttenthaler@cbs.mpg.de)

Martin, M.N.H, Hebart; [hebart@cbs.mpg.de](mailto:hebart@cbs.mpg.de)

## Abstract

Over the past decade, deep neural network (DNN) models have received a lot of attention due to their near-human object classification performance and their excellent prediction of signals recorded from biological visual systems. To better understand the function of these networks and relate them to hypotheses about brain activity and behavior, researchers need to extract the activations to images across different DNN layers. The abundance of different DNN variants, however, can often be unwieldy, and the task of extracting DNN activations from different layers may be non-trivial and error-prone for someone without a strong computational background. Thus, researchers in the fields of cognitive science and computational neuroscience would benefit from a library or package that supports a user in the extraction task. **THINGSvision** is a new Python module that aims at closing this gap by providing a simple and unified tool for extracting layer activations for a wide range of pretrained and randomly-initialized neural network architectures, even for users with little to no programming experience. We demonstrate the general utility of **THINGSvision** by relating extracted DNN activations to a number of functional MRI and behavioral datasets using representational similarity analysis, which can be performed as an integral part of the toolbox. Together, **THINGSvision** enables researchers across diverse fields to extract features in a streamlined manner for their custom image dataset, thereby improving the ease of relating DNNs, brain activity, and behavior, and improving the reproducibility of findings in these research fields.

**Keywords:** Deep Neural Networks, Computational Neuroscience, Computer Vision, Feature extraction, Artificial Intelligence, Python

**Author roles:** Conceptualization: L.M. & M.N.H; Funding acquisition: M.N.H.; Resources: L.M. & M.N.H.; Software: L.M.; Supervision: M.N.H.; Visualization: L.M.; Writing – original draft: L.M.; Writing – final manuscript: L.M. & M.N.H.

## 1 Introduction

In recent years, deep neural networks (DNNs) have sparked a lot of interest in the related fields of cognitive science, computational neuroscience, and artificial intelligence. This is mainly owing to their power as arbitrary function approximators ([LeCun, Bengio, & Hinton, 2015](#)), their

near-human performance on object recognition and natural language understanding tasks (e.g., Russakovsky et al. (2015); Wang et al. (2019, 2018)), and, most crucially, the fact that their latent representations often show a close correspondence to brain recordings and behavioral measurements (Güçlü & van Gerven, 2014; Khaligh-Razavi & Kriegeskorte, 2014; Kietzmann, McClure, & Kriegeskorte, 2018; King, Groen, Steel, Kravitz, & Baker, 2019; Kriegeskorte, 2015; Schrimpf et al., 2018, 2020; Yamins et al., 2014).

One important limiting factor for a much broader interdisciplinary adoption of DNNs as computational models lies in the difficulty of extracting layer activations for DNNs. This difficulty is twofold. First, the number of existing models is enormous and increases by the day. Due to this diversity, an extraction strategy that is suited for one model may not apply to any other model. Second, for users without a strong programming background it can be non-trivial to extract features while being confident that no mistakes were made in the process, for example during image preprocessing, layer selection, or image-activation correspondence. Together, this demonstrates that researchers in cognitive science and computational neuroscience would benefit from a readily-available package for a streamlined extraction of neural network activation.

With **THINGSvision**, we provide a Python toolbox that enables researchers to extract features for most state-of-the-art neural network models for existing or custom image datasets with just a few lines of code. In the remainder of this article, we introduce and motivate the main functionalities of the library and how to use them. We start by providing an overview of the collection of neural network models for which features can be extracted. The code for **THINGSvision** is publicly available: <https://github.com/ViCCo-Group/THINGSvision>.

## 1.1 Model collection

All neural network models that are part of **THINGSvision** are built in PyTorch (Paszke et al., 2019), which is one of the most common deep learning frameworks. We include every neural network model that is part of PyTorch’s publicly available model-zoo, **torchvision**, including many DNN models commonly used in research such as AlexNet (Krizhevsky, Sutskever, & Hinton, 2012), VGG-16 (Simonyan & Zisserman, 2015), and ResNet (He, Zhang, Ren, & Sun, 2016). Whenever a new architecture is added to **torchvision**, **THINGSvision** is designed to automatically make it available, as well.

In addition to models from the **torchvision** library, we provide both feedforward and recurrent variants of CORnet, a recent DNN model that was inspired by the architecture of the non-human primate visual system and that leverages recurrence to more closely resemble biological processing mechanisms (Kubilius et al., 2019, 2018). At the time of writing, CORnet-S is the best performing computational model on the BrainScore benchmark (Schrimpf et al., 2018, 2020), a composition of various neural and behavioral benchmarks aimed at assessing the degree to which a DNN is a good model of cortical visual object processing.

Moreover, we include both versions of CLIP (Radford et al., 2021), a multimodal DNN model developed by OpenAI that is based on the Transformer architecture (Vaswani et al., 2017), which has surpassed the performance of previous recurrent and convolutional neural networks on a wide range of core natural language processing and image recognition tasks. CLIP’s training procedure makes it possible to simultaneously extract both image and text features for visual concepts and their natural language counterparts. CLIP exists as an advanced, multimodal version of ResNet50 (He et al., 2016) and the so-called Vision-Transformer, ViT (Dosovitskiy et al., 2020).

To facilitate the reproducibility of computational analyses across research groups and fields, it is crucial to not only make code pertaining to the proposed analysis pipeline publicly available but additionally offer a general and well documented framework that can easily be adopted by others (Esteban et al., 2018; Peng, 2011; Rush, 2018; Van Lissa et al., 2020). This is why we aspired to follow high software engineering principles during development. We view **THINGSvision**

as a toolbox that aims at promoting both the interpretability and comparability of research at the intersection of cognitive science, computational neuroscience, and artificial intelligence. Instead of simply providing an unwieldy collection of existing computational models in the realm of computer vision, we decided to focus on models whose functional composition has been demonstrated to be similar to the primate visual system (Kietzmann et al., 2018; Kriegeskorte, 2015) and models that are widely adopted by the community.

## 2 Method

THINGSvision is a toolbox that was written in the high-level programming language Python and, therefore, requires the most recent Python 3 version to be installed on a user's machine. The toolbox leverages two of the most widely used packages in the context of machine learning research and numerical analysis, namely PyTorch (Paszke et al., 2019) and NumPy (Harris et al., 2020). Since all relevant NumPy operations were made an integral part of THINGSvision, it is not necessary to import NumPy or any other Python package explicitly.

To extract features from a neural network model for a custom set of images, users are first required to select a model and additionally define whether the model's weights were pretrained on ImageNet (Deng et al., 2009; Russakovsky et al., 2015) or randomly initialized. Second, input and output folders as well as the number of samples to be processed in parallel in so-called mini-batches are passed to a function that converts the user's images into a PyTorch dataset. This dataset subsequently serves as the input to a function that extracts features for the selected module (e.g., the penultimate layer). The above operations are performed with the following lines of code, which essentially encompass the basic flow of THINGSvisions's extraction pipeline

```
import thingsvision.vision as vision

model, transforms = vision.load_model('alexnet', pretrained=True, device='cuda')
data_loader = vision.load_dl(root='./images/', out_path='./alexnet/features.10/features/',
                             batch_size=64, transforms=transforms)
features, targets = vision.extract_features(model, data_loader, 'features.10',
                                             batch_size=64, flattenActs=True, device='cuda')

vision.save_features(features, out_path='./alexnet/features.10/features/.npy')
```

Note that at this point it appears crucial to stress the difference between a layer and a module. Module is a more general reference to the individual parts of a model. A module can refer to non-linearities, pooling operations, batch normalization and convolutional or fully-connected layers, whereas a layer usually refers to an entire model block, such as the composition of the latter set of modules or a single layer (e.g., fully-connected or convolutional). We will, however, use the two terms interchangeably in the remainder of this article whenever a module refers to a layer. Moreover, extracting features is used interchangeably with extracting network activations.

Figure 1 depicts a high-level overview of how feature extraction is streamlined in THINGSvision. Given that a user provides the system path to an image dataset, the input to a neural network model is a three-dimensional matrix,  $I \in \mathbb{R}^{H \times W \times C}$ , which is the numerical representation of any image. Assuming that a user wants to apply the flattening operation to the activations from the selected module, the output corresponding to each input is a one-dimensional vector,  $z \in \mathbb{R}^{KHW}$ .

In the following paragraphs, we will explain both operations and the variables necessary for feature extraction in more detail. We start by introducing variables that we deem helpful for structuring the extraction workflow.

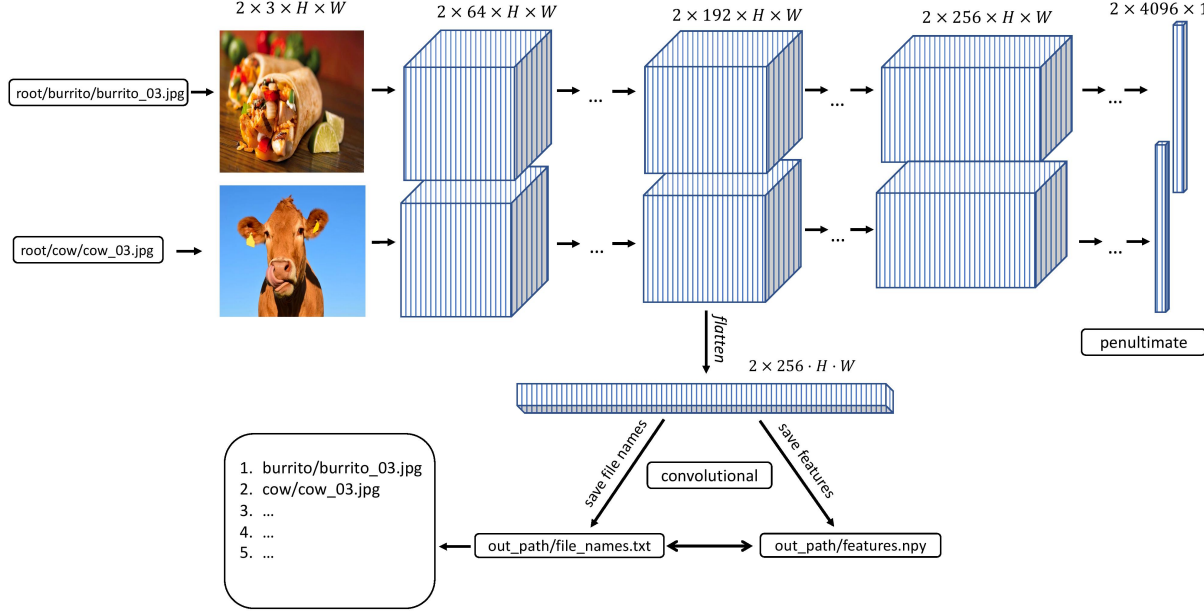


**Figure 1:** THINGSvision feature extraction pipeline for an example convolutional neural network architecture. In this example the batch size  $B$  is set to two, and the image dimensions are permuted.

## 2.1 Variables

Variable	Example assignment	Short description
root (str)	'./images/'	system directory where a user's image set is stored
model_name (str)	'alexnet'	name of the neural network model
pretrained (bool)	True	pretrained or random weights
batch_size (int)	64	number of image samples per mini-batch
module_name (str)	'features.10'	part of the model from which to extract features
out_path (str)	f'{root}/{model_name}/{module_name}/'	location on machine where to store features
file_format (str)	'.npy'	format in which to store features
device (str)	'cuda'	whether to perform feature extraction on GPU or CPU

**Figure 2:** Overview of the global variables that are relevant for THINGSvision's feature extraction pipeline and that facilitate a user's workflow.

Before leveraging THINGSvision's full functionality, a user is advised to assign values to seven global variables, which, for simplicity, we define as their corresponding keyword argument names: `root`, `model_name`, `pretrained`, `batch_size`, `out_path`, `file_format`, and `device`. Note that this is not a necessity, since the values pertaining to those variables can simply be passed as input arguments to the respective functions. It does, however, facilitate the ease of reading, and in our opinion clearly contributes to a better workflow. Moreover, there is the option to additionally assign a value to the variable `module_name` whose significance we will explain in Section 2.2.2. The above variables, their data types, example assignments, and short descriptions are displayed in Figure 2. We will explain the details of these variables in the remainder of this section. More advanced users can simply jump to Section 2.2.

### 2.1.1 Root

We recommend starting with the assignment of the `root` variable. This variable is supposed to correspond to the system directory where a user's image set is stored.

```
root = './images/'
```

### 2.1.2 Model name

Next, a user is required to specify the name of the neural network model whose features corresponding to the images in `root` ought to be extracted. The model's name can be defined as one of the available neural network models in `torchvision`. Conveniently, as soon as a new model is added to `torchvision`, it will also be included in `THINGSvision`, since we inherit from `torchvision`. For simplicity, we use `alexnet` throughout the remainder of the article, as shown in Figure 2.

```
model_name = 'alexnet'
```

### 2.1.3 Pretrained

As a subsequent step, a user needs to specify whether to load a pretrained model (i.e., pretrained on `ImageNet`) into memory, or whether to solely load the parameters of a model that has not yet been trained on any publicly available dataset (so-called randomly initialized networks). The latter may be relevant for architectural comparisons when one is concerned not with the knowledge of a model but with its architecture. In the current example, we assume that the user is interested in a model's knowledge and not its function composition, which is why we set the variable `pretrained` to `true`. Note that `pretrained` must be assigned with a Boolean value (see Figure 2).

```
pretrained = True
```

### 2.1.4 Batch size

Modern neural network architectures process several images at a time in batches. To make the extraction of neural network activations more time efficient, `THINGSvision` follows this processing choice, sampling  $B$  images in parallel. Thus, the choice of the user lies in the trade-off between processing time and memory usage (GPU memory or RAM). For users who are not concerned with extraction speed, we recommend setting  $B$  to 32. In our example  $B$  is set to 64 (see Figure 2)

```
batch_size = 64
```

### 2.1.5 Device

A user can choose between using a CPU and a GPU if a GPU is available. The advantage of leveraging a GPU lies in its faster computation. Note that GPU usage is possible only if a machine is equipped with an NVIDIA GPU.

```
device = 'cuda' if torch.cuda.is_available() else 'cpu'
```

### 2.1.6 Module name

`Module_name` refers to the part of the model from which network activations should be extracted. In case a user is familiar with the architecture of the neural network model for which features should be extracted, the variable `module_name` can be set manually (e.g., `features.10`). There is, however, the possibility to first inspect the model architecture through an additional function call, and subsequently select a module based on the output of this function. The function prompts a user to select a module, which is then assigned to `module_name` in the form of a string. In Section 2.2.2, we will explain in more detail how this can be done.

```
module_name = 'features.10'
```

### 2.1.7 Output directory

Before saving features to disk, a user is required to specify the directory where image features should be stored. For simplicity, in Figure 2 we define `out_path` as a succession of previously defined variables.

```
out_path = f'./{root}/{model_name}/{module_name}/'
```

### 2.1.8 File format

A user can specify the `file_format` in which the image features are stored. This variable can be set either to `.txt`, `.mat` or `.npy`. If subsequent analyses are performed in Python, we recommend to set `file_format` to `.npy`, as storing large matrices in `.npy` format is both more memory and time efficient than doing the same in `.txt` format. This is due to the fact that `.npy` formats were specifically designed to accommodate the storing of large matrices to NumPy (Harris et al., 2020).

```
out_path = '.npy'
```

## 2.2 Model & modules

### 2.2.1 Loading models

With the previously defined variables in place, a user can now start loading a model into a computer's memory. Since `model_name` is set to `alexnet` and `pretrained` to `true`, we load an AlexNet model pretrained on ImageNet and the corresponding image transformations (which are used in 2.3) into memory with the following line,

```
model, transforms = vision.load_model(model_name, pretrained=pretrained, device=device)
```

### 2.2.2 Selecting modules

Before extracting DNN features for an image dataset, a user is required to select the part of the model for which features should be extracted. In case a user is familiar with the architecture of a specific neural network model, they can simply assign a value to the variable `module_name` (see Section 2.1.6). If a user is, however, unfamiliar with the specific architecture of a neural network model, we recommend visualizing the composition of the model's modules through the following function call,

```
module_name = vision.show_model(model, model_name)
```

The output of this call, in the case of `alexnet`, looks as follows,

```
AlexNet(  
    (features): Sequential(  
        (0): Conv2d(3, 64, kernel_size=(11, 11), stride=(4, 4), padding=(2, 2))  
        (1): ReLU(inplace=True)  
        (2): MaxPool2d(kernel_size=3, stride=2, padding=0, dilation=1, ceil_mode=False)  
        (3): Conv2d(64, 192, kernel_size=(5, 5), stride=(1, 1), padding=(2, 2))  
        (4): ReLU(inplace=True)  
        (5): MaxPool2d(kernel_size=3, stride=2, padding=0, dilation=1, ceil_mode=False)  
        (6): Conv2d(192, 384, kernel_size=(3, 3), stride=(1, 1), padding=(1, 1))  
        (7): ReLU(inplace=True)  
        (8): Conv2d(384, 256, kernel_size=(3, 3), stride=(1, 1), padding=(1, 1))  
        (9): ReLU(inplace=True)  
        (10): Conv2d(256, 256, kernel_size=(3, 3), stride=(1, 1), padding=(1, 1))  
        (11): ReLU(inplace=True)  
        (12): MaxPool2d(kernel_size=3, stride=2, padding=0, dilation=1, ceil_mode=False)  
    )  
    (avgpool): AdaptiveAvgPool2d(output_size=(6, 6))  
    (classifier): Sequential(  
        (0): Dropout(p=0.5, inplace=False)  
        (1): Linear(in_features=9216, out_features=4096, bias=True)  
        (2): ReLU(inplace=True)  
        (3): Dropout(p=0.5, inplace=False)  
        (4): Linear(in_features=4096, out_features=4096, bias=True)  
        (5): ReLU(inplace=True)  
        (6): Linear(in_features=4096, out_features=1000, bias=True)  
    )  
)
```

For users unfamiliar with details of neural network architectures, this output may look confusing, given that it is well known that AlexNet consists only of 8 layers. Note, however, that the above terminal output displays the individual modules of AlexNet as well as their specific attributes, such as how many features their inputs and outputs have, or whether a layer is followed by a rectifier non-linearity or pooling operation. Note further that the modules are enumerated in the order in which they appear within the model's composition. This is crucial for the module selection step. During this step, THINGSvision prompts a user to "enter the part of the model for which a user would like to extract image features". The user's input is automatically assigned to the variable `module_name` in the form of a string. In order to extract features from layers that correspond to early areas of the primate visual system, we recommend selecting convolutional or pooling modules, and linear layers for later areas that encode high-level features.

It is important to stress that each model in PyTorch is represented by a tree structure, where the name of the model refers to the root of the tree (e.g., AlexNet). To access a module, a user is required to compose the string variable `module_name` by both the name of one of the leaves that directly follow the tree's root (e.g., `features`, `avgpool`, `classifier`) and the number of the module to be selected, separated by a period (e.g., `features.5`). This approach to module selection accounts for all models that are part of THINGSvision.

In this example, we select the 10<sup>th</sup> module of AlexNet's leaf `features` (i.e., `features.10`), which corresponds to the fifth convolutional layer in AlexNet (see above). Hence, features will be extracted exclusively for this module.

## 2.3 Dataset & Data loader

Through a dedicated dataset class, THINGSvision can deal with various types of image data (`.eps`, `.jpg`, `.jpeg`, `.png`, `.PNG`, `.tif`, `.tiff`) and is able to transform the images into a ready-to-use PyTorch dataset. System paths to images can follow the folder structure `./root/class/img_xy.png`

or `./root/img_xy.png`, where the former directory contains sub-folders for the respective image classes. A dataset is subsequently wrapped with a PyTorch iterator to enable batch-wise feature extraction. The above is done with,

```
dl = vision.load_dl(root, out_path=out_path, batch_size=batch_size, transforms=transforms)
```

`THINGSvision` automatically sorts image files alphabetically (i.e., A-Z or 0-9). Sorting, however, depends on a machine's operating system. An alphabetic sort differs across DOS, Unix, and Linux, which is why we provide the possibility to sort the data according to a list of file names, manually defined by the user. The features will, subsequently, be extracted in the order of the provided file names.

This list must follow the `List[str]` data structure (i.e., containing `strings`), such as `[aardvark/aardvark_01.jpg, aardvark/aardvark_02.jpg, ...]` or `[aardvark.jpg, anchor.jpg, ...]`, depending on whether the dataset tree consists of subfolders for classes (see above). The list of file names can be passed as an optional argument as follows,

```
data_loader = vision.load_dl(root, out_path=out_path, batch_size=batch_size,\n                             transforms=transforms, file_names=file_names)
```

We use the variable `dl` here since it is a commonly used abbreviation for "data loader". It is, moreover, necessary to pass `out_path` to the above function to save a `.txt` to `out_path` consisting of the image names in the order in which features are extracted. This is done to ensure that a user can easily correspond the rows of a feature matrix to the image names, as shown in Figure 1.

## 2.4 Features

The following section is meant for readers curious to understand what is going on under the hood of `THINGSvision`'s feature extraction pipeline and, additionally, who aim to get a better grasp of the dimensions depicted in Figure 1. Readers who are familiar with matrices and tensors may want to skip this section and jump directly to Section 2.4.2, since the following paragraphs are not crucial for using the toolbox. We use mathematical notation to denote images (inputs) and features (outputs).

### 2.4.1 Extracting features

When all variables necessary for feature extraction are set, the user can extract image features for a specific (here, the fifth convolutional) layer in AlexNet (i.e., `features.10`). Figure 1 shows `THINGSvision`'s feature extraction pipeline for two example images. The algorithm first searches for the images in the `root` folder, subsequently converts them into a ready-to-use dataset, and then passes sub-samples of the data in the form of mini-batches as inputs to the network. For simplicity and to demonstrate the extraction procedure, Figure 1 displays an example of a simplified convolutional neural network architecture. Recall that an image is numerically represented as a three-dimensional array, usually in the following format

$$I \in \mathbb{R}^{H \times W \times C}, \quad (1)$$

where  $H$  = height,  $W$  = width,  $C$  = channels.  $C = 1$  or  $3$ , depending on whether images are represented in grayscale or RGB format. In PyTorch, however, image batches, denoted as  $X$ , are represented as four-dimensional tensors,

$$X \in \mathbb{R}^{B \times C \times H \times W}, \quad (2)$$

where  $B = \text{batch\_size}$ , and all other dimensions are permuted. In the example in Figure 1,  $B = 2$ , since two images are concurrently processed. The channel dimension, now, represents the tensor's second dimension (inside the toolbox, it is the first dimension, since Python starts indexing at 0) to more easily apply convolutions to input images. Hence, features at the level of the selected module, denoted as  $Z$ , are represented as four-dimensional tensors in the format,

$$Z \in \mathbb{R}^{B \times K \times H \times W}, \quad (3)$$

where the channel parameter  $C$  is replaced with  $K$  referring to the number of feature maps within a representation. Here,  $K = 256$ , and  $H$  and  $W$  are significantly smaller than at the input level. For most analyses in computational neuroscience, researchers are required to flatten this four-dimensional tensor into a two-dimensional matrix of the format,

$$Z_{\text{flat}} \in \mathbb{R}^{B \times KHW}, \quad (4)$$

i.e. one vector per image representation in a batch, which is what we demonstrate in the following example. We provide a keyword argument, called `flatten_acts`, that communicates to the function to automatically perform the previous step during feature extraction (see the `flatten` operation in Figure 1). A user must simply set the argument to `True` as follows,

```
features, targets = vision.extract_features(model, dl, module_name, \
                                             batch_size=batch_size, flatten_acts=True, device=device)
```

The final, two-dimensional, feature matrix is of the form,

$$Z_{\text{flat}} \in \mathbb{R}^{N \times KHW}, \quad (5)$$

where  $N$  corresponds to the number of images in the dataset. In addition to the feature matrix, `extract_features` returns a target vector of size  $N \times 1$  corresponding to the image classes. A user can decide whether to save or ignore this target vector, depending on the subsequent analyses. Note that flattening a tensor is not necessary for feature extraction to work. If a user wants the original four-dimensional tensor, `flatten_acts` must be set to `False`. To offer a user more flexibility and control over the feature extraction procedure, we do not provide a default value for this keyword argument. Since it is non-trivial to store a four-dimensional tensor with NumPy or PyTorch to disk, THINGSvision comes (1) with a function that slices a four-dimensional tensor into multiple two-dimensional matrices, and (2) a corresponding function that merges the slices back into their original shape at the time of loading the features back into memory.

#### 2.4.2 Saving features

To save network activations (no matter from which part of the model) in a flattened format, the following function can be called,

```
vision.save_features(features, out_path, file_format)
```

When features are extracted from any of the non-linear layers (e.g., convolutional, batch normalization, pooling), the output is a four-dimensional tensor (see Equation 3). Since four-dimensional tensors cannot be saved to disk easily, they must be sliced into different sub-matrices in the form of `.txt` files. To save the output without performing the flattening operation on the features,  $Z$ , execute

```
vision.tensor2slices(out_path, 'features', features)
```

Recall that `flatten_acts` must be set to `False` to perform the above operation. Slicing a four-dimensional array into multiple two-dimensional matrices can, unfortunately, not be achieved easily in `.npy` format, which is why we do not provide a `file_format` argument for `tensor2slices`. To load the slices back into memory in their original four-dimensional tensor format, a user must simply make the following call,

```
features = vision.slices2tensor(out_path, 'features'),
```

where

$$Z = \mathbb{R}^{N \times K \times H \times W} \quad (6)$$

When storing network activations from non-linear layers in their flattened format, it is possible to run into `MemoryErrors`. We account for that potential caveat with splitting two-dimensional matrices into  $k$  equally large splits, whenever that happens. The default value of  $k$  is set to 10. If 10 splits are not sufficient to counteract the memory issues, a user can change this value to a larger number. We recommend trying multiples of 10, such as

```
vision.save_features(features, out_path, file_format, n_splits=20)
```

To merge the array splits back into a single, two-dimensional, feature matrix, a user can call,

```
features = vision.merge_features(out_path, file_format)
```

## 3 Applications & Results

To demonstrate the usefulness of `THINGSvision`, in the following, we present analyses of the image representations of different deep neural network architectures and compare them against representations obtained from behavioral experiments (3.2.1) and functional MRI responses to higher visual cortex (3.2.2). To qualitatively inspect the representations embedded in the extracted DNN activations, we compute and visualize representational dissimilarity matrices (RDMs) within the framework of representational similarity analysis (RSA). Moreover, we calculate the Pearson correlation coefficients between human and DNN representations to quantify their similarities, and show how this can easily be done with `THINGSvision`. We start by briefly introducing RSA and motivating its application.

### 3.1 Representational Similarity Analysis

Representational Similarity Analysis (RSA), a technique that originated in cognitive computational neuroscience, can be used to relate object representations from different measurement modalities (e.g., fMRI or behavior) and different computational models with each other (Kriegeskorte, Mur, & Bandettini, 2008; Kriegeskorte, Mur, Ruff, et al., 2008). RSA is based on representational dissimilarity matrices (RDMs), which capture the representational geometry present in a given system (e.g., in the brain or a DNN), thereby abstracting away from the underlying multivariate pattern. Rather than directly comparing measurements, RDMs compare representational similarities between two systems. RDMs are symmetric, square matrices, where the rows and columns are indexed by the different conditions or objects. Hence, RSA is a convenient analysis tool to compare visual object representations obtained from different DNNs.

The dissimilarity between each object pair (e.g., two images) is computed within the row space of an RDM. Dissimilarity is quantified as the distance between two objects in the measured representational space, defined by the chosen distance metric. The user can choose between the Euclidean distance (`euclidean`), the correlation distance (`correlation`), the cosine distance (`cosine`) and a radial basis function applied to pairwise distances (`gaussian`). Equivalent object

representations show a dissimilarity score close to 0. For the **correlation** and **cosine** distances, the maximum dissimilarity score is bounded to 2, whereas there is no theoretical upper limit for the **euclidean** distance.

Since RDMs are symmetric around their main diagonal, it is simple to compare them by correlating their lower or upper triangles. We include both the possibility to compute and visualize an RDM and to correlate the upper triangles of two distinct RDMs. Computing an RDM based on a Pearson correlation distance matrix is as simple as calling

```
rdm = vision.compute_rdm(features, method='correlation'),
```

Note that similarities are computed between conditions or objects, not features. To compute the representational similarity between two distinct RDMs, a user can make the following call,

```
rdm_correlation = vision.correlate_rdms(rdm_1, rdm_2, correlation='pearson')
```

The default **correlation** value is the Pearson correlation coefficient, but this can be changed to **spearman** if a user assumes that the similarities are not ratio scale and require the computation of a Spearman rank correlation (Arbuckle, Yokoi, Pruszynski, & Diedrichsen, 2019; Nili et al., 2014). To visualize an RDM and automatically save the output image (in .png or .jpg format) to disk, one may call

```
vision.plot_rdm(out_path, features, method='correlation',  
format='.png', colormap='cividis', show_plot=True)
```

The default value of **format** is set to .png but can easily be changed to .jpg. Note that .jpg is a lossy image compression, whereas .png is lossless, and, hence, with .png no information gets lost during compression. Therefore, the **format** argument influences both the size and the final resolution of the RDM image representation. The **dpi** value is set to 200 to guarantee for a high image resolution, even if .jpg is selected.

## 3.2 The penultimate layer

The correspondence of a DNN’s penultimate layer to human behavioral representations has been studied extensively and is therefore often used when investigating the representations of abstract visual concepts in neural network models (e.g., Bankson et al., 2018; Battleday, Peterson, & Griffiths, 2019; Cichy, Kriegeskorte, Jozwik, van den Bosch, & Charest, 2019; Jozwik, Kriegeskorte, Cichy, & Mur, 2018; Mur et al., 2013; Peterson, Abbott, & Griffiths, 2018). To the best of our knowledge, our study is the first to compare visual object representations extracted from CLIP (Radford et al., 2021) against the representations of well known vision models that have previously shown a close correspondence to neural recordings of the primate visual system. We computed RDMs based on the Pearson correlation distance for seven models, namely AlexNet (Krizhevsky et al., 2012), VGG16 and VGG19 with batch normalization (Simonyan & Zisserman, 2015), which show a close correspondence to brain and behavior (Schrimpf et al., 2018, 2020), ResNet50 (He et al., 2016), BrainScore’s current leader CORnet-S (Kubilius et al., 2019, 2018; Schrimpf et al., 2020), and OpenAI’s CLIP variants CLIP-RN and CLIP-ViT (Radford et al., 2021). The comparison was done for six different image datasets that included functional MRI of the human visual system and behavior (Bankson et al., 2018; Cichy et al., 2019; Hebart et al., 2020; Mohsenzadeh et al., 2019; Mur et al., 2013).

Note that Bankson et al. (2018) exploited two different datasets which we label with ”(1)” and ”(2)” in Figure 3. The number of images per dataset are as follows: (Cichy, Pantazis, & Oliva, 2014; Kriegeskorte, Mur, Ruff, et al., 2008; Mur et al., 2013): 92; (Bankson et al., 2018) 84 each; (Cichy, Khosla, Pantazis, Torralba, & Oliva, 2016; Cichy et al., 2019): 118; (Mohsenzadeh et al., 2019): 156; (Hebart et al., 2019, 2020): 1854. For each of these datasets except for Mohsenzadeh

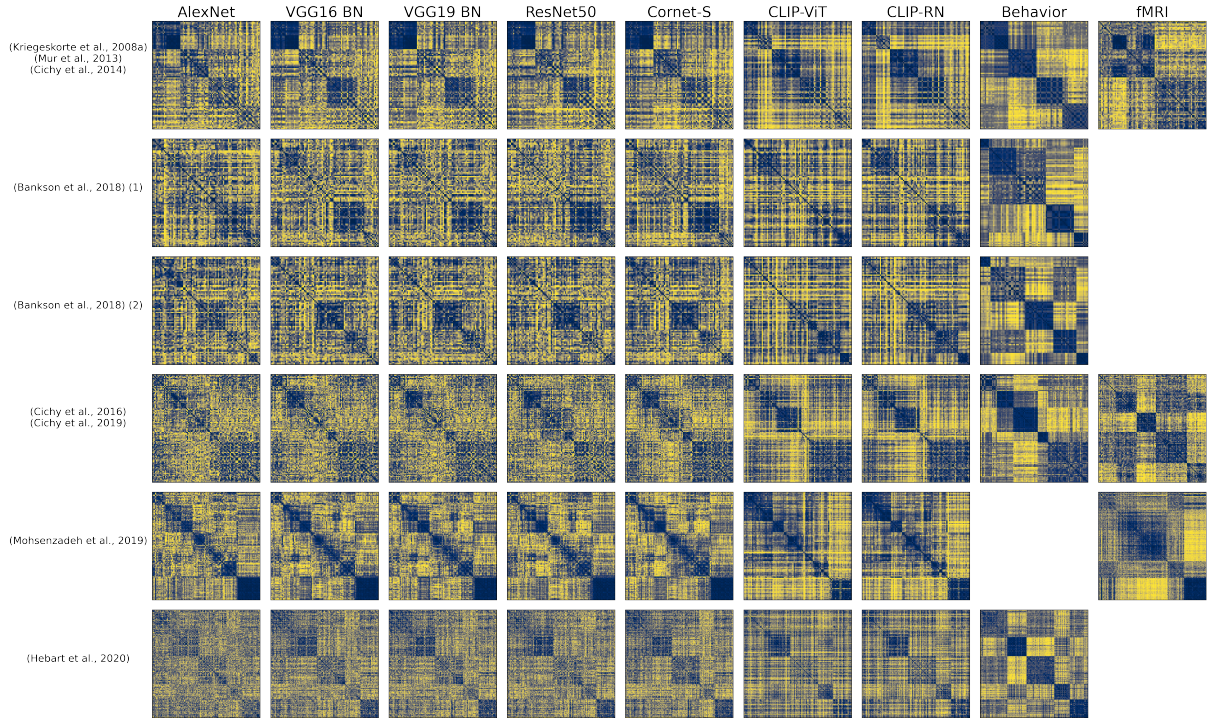


**Figure 3:** RDMs for representations of the penultimate layer of different neural network models (with pretrained weights), for group averages of behavioral judgments, and for fMRI responses to higher visual cortex. For [Mohsenzadeh et al. \(2019\)](#), no behavioral experiments had been conducted. For both datasets in [Bankson et al. \(2018\)](#), and for [Hebart et al. \(2020\)](#), no fMRI recordings were available. For display purposes, [Hebart et al. \(2020\)](#) was downsampled to 200 conditions. RDMs were reordered according to an unsupervised clustering.

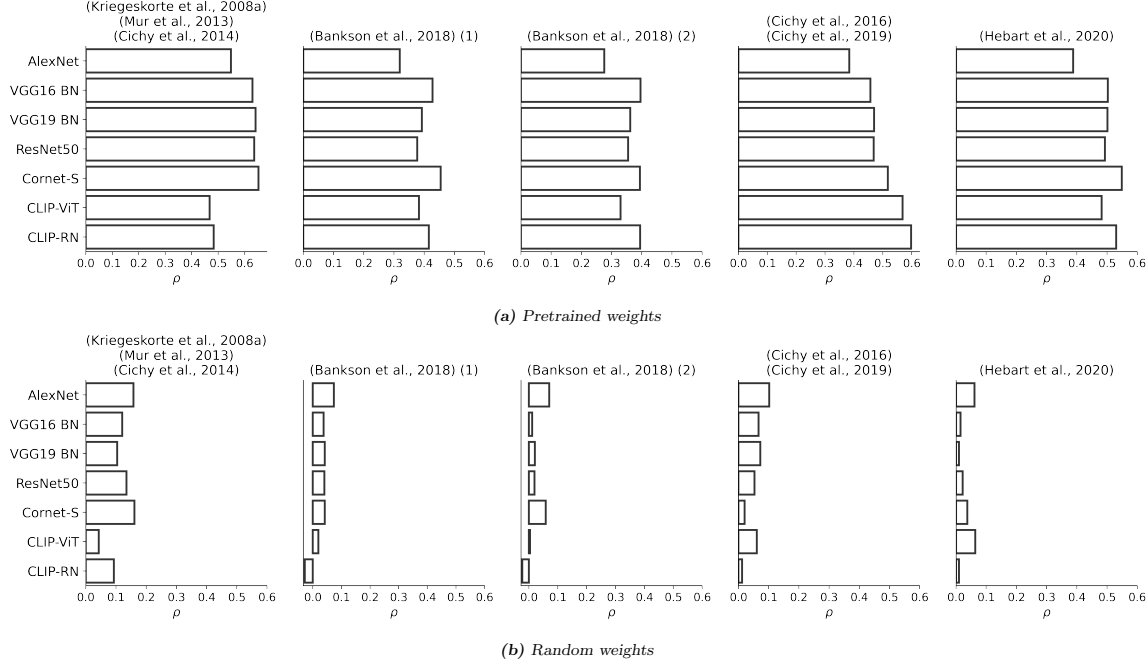
[et al. \(2019\)](#), we additionally computed RDMs for group averages obtained from behavioral experiments. Furthermore, we computed RDMs for brain voxel activities obtained from fMRI recordings for the datasets used in [Cichy et al. \(2014\)](#), [Cichy et al. \(2016\)](#), and [Mohsenzadeh et al. \(2019\)](#), based on voxels inside a mask covering higher visual cortex.

Figure 3 visualizes all RDMs. We clustered RDMs pertaining to group averages of behavioral judgments into five object clusters and sorted the RDMs corresponding to object representations extracted from DNNs according to the obtained cluster labels. The image datasets used in [Cichy et al. \(2014\)](#); [Kriegeskorte, Mur, Ruff, et al. \(2008\)](#); [Mur et al. \(2013\)](#) and [Mohsenzadeh et al. \(2019\)](#) were already sorted according to object categories, which is why we did not perform a clustering on RDMs for those datasets. The cluster size was chosen arbitrarily. This reordering was mainly done to highlight the similarities and differences in RDMs.

### 3.2.1 Behavioral correspondences

**Pretrained weights** Across all compared DNN models, CORnet-S and CLIP-RN showed the overall closest correspondence to behavioral representations. CORnet-S, however, was the only model that performed well across all datasets. CLIP-RN showed a high Pearson correlation (ranging from 0.40 to 0.60) with behavioral representations across most datasets, with [Mur et al. \(2013\)](#) being the only exception, for which both CLIP versions performed poorly. Interestingly, for one of the datasets in [Bankson et al. \(2018\)](#), VGG16 with batch normalization ([Simonyan & Zisserman, 2015](#)) outperformed both CORnet-S and CLIP-RN (see Figure 4 (a)). AlexNet consistently performed the worst for behavioral fits. Note that the broadest coverage of visual stimuli is provided by [Hebart et al. \(2019, 2020\)](#), which should therefore be seen as the most representative result (rightmost column in Figure 4).

**Random weights** Another interesting finding is that for randomly-initialized weights, CLIP-RN is the poorest performing model in four out of five datasets (see Figure 4 (b)). Here, AlexNet seems to be the best performing model across datasets, although it achieved the lowest correspondence to behavioral representations when leveraging a pretrained version (see Figure 4 (a))). This indicates the possibility of complex interactions between model architectures and training objectives that require further investigations.



**Figure 4:** Pearson correlation coefficients for comparisons between neural network and behavioral representations. Upper row: Network activations extracted from pretrained models. Bottom row: Network activations extracted from randomly initialized models.

### 3.2.2 Brain correspondences

We performed a similar analysis as above, but this time leveraging RDMs corresponding to fMRI responses to examine the correlation between model and brain representations of higher visual cortex. We first report results obtained from analyses with pretrained models.

**Pretrained weights** While AlexNet (Krizhevsky et al., 2012) showed the worst correspondence to human behavior in four out of five datasets (see Figure 4 (a)), AlexNet correlated strongly with representations extracted from fMRI responses to higher visual cortex, except for the dataset used in Cichy et al. (2016) (see Figure 3 (a)). This is interesting, given that among the entire set of analyzed deep neural network models AlexNet shows the poorest performance on ImageNet (Russakovsky et al., 2015). This result contradicts findings from previous studies arguing that object recognition performance is correlated with correspondences to fMRI recordings (Schriftpf et al., 2020; Yamins et al., 2014). This time, CORnet-S and CLIP-RN performed well for the datasets used in Cichy et al. (2016) and in Mohsenzadeh et al. (2019), but were among the poorest performing DNNs for Cichy et al. (2014). Note, however, that the dataset used in Cichy et al. (2014) is highly structured and contains a large number of faces and similar images, something AlexNet might pick up more easily in its image features but something that is not reflected in human behavior (Grootswagers & Robinson, 2021).

**Random weights** When comparing representations corresponding to network activations from models with random weights, there appears to be no consistent pattern as to which model

correlated most strongly with brain representations of higher visual cortex, although VGG16 and CORnet-S were the only two models that yielded a positive Pearson correlation coefficient across datasets. Note, however, that for each model we extracted network activations from the penultimate layer. Results might look different when extracting activations from earlier layers of the networks or when reweighting the DNN features prior to RSA ([Kaniuth & Hebart, 2020](#); [Storrs, Khaligh-Razavi, & Kriegeskorte, 2020](#)). We leave further investigations to future studies, as our analyses should only demonstrate the applicability of our toolbox.

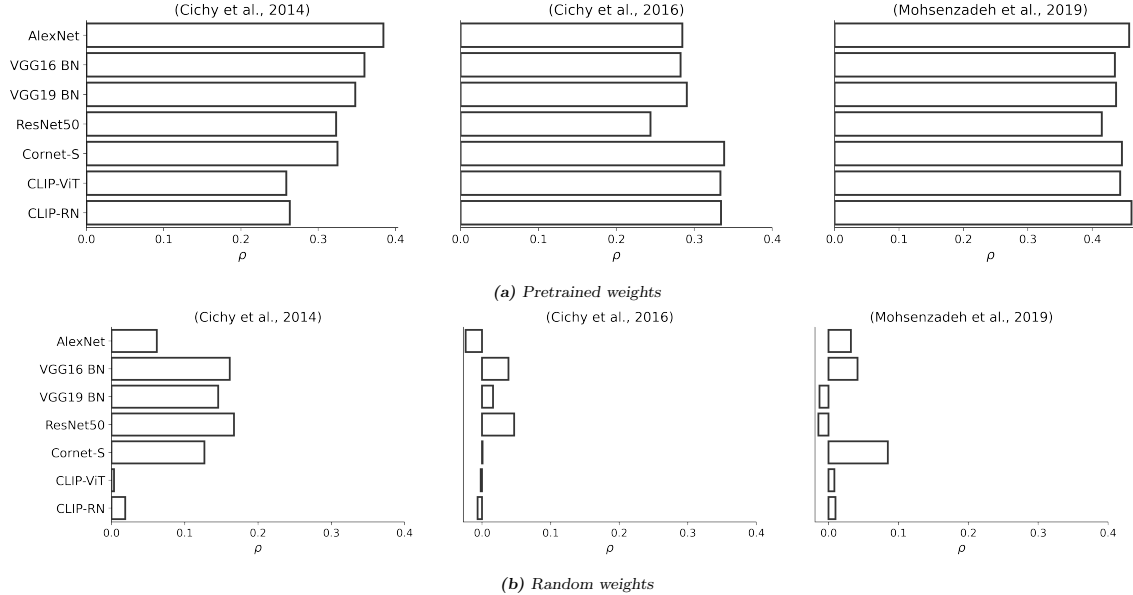


**Figure 5:** Pearson correlation coefficients for comparisons between neural network representations extracted from the penultimate layer and representations corresponding to fMRI responses of higher visual cortex. Upper row: Network activations extracted from pretrained models. Bottom row: Network activations extracted from models with random weights.

### 3.2.3 Model comparison

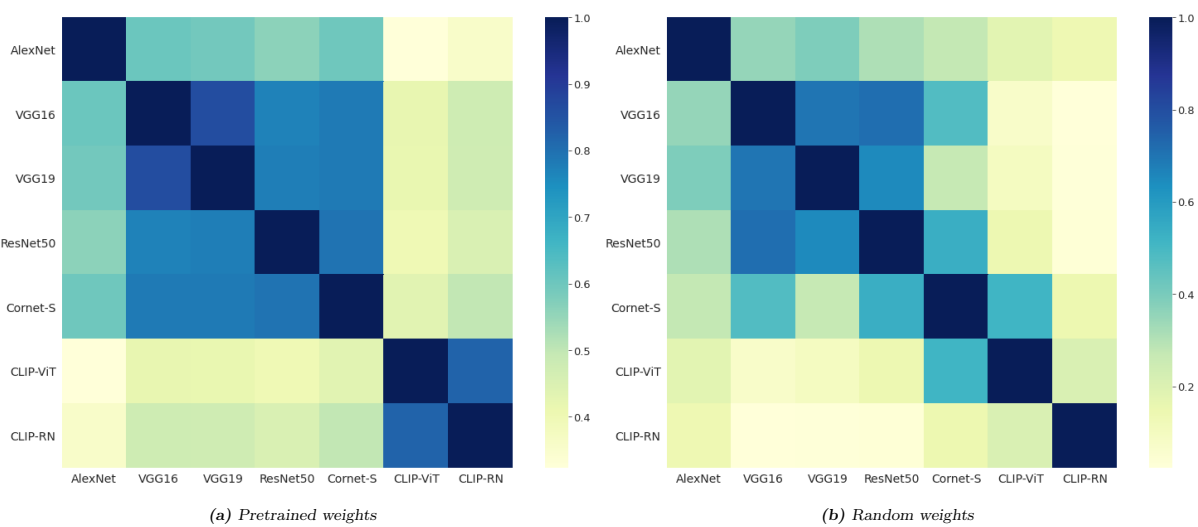


**Figure 6:** RSA across models (Second-order RSA). Pearson correlation coefficients between penultimate layer representations for the THINGS image dataset ([Hebart et al., 2019](#)). For each model combination, we compared the flattened upper triangular of each model's RDM.

Although CORnet-S and CLIP-RN achieved the overall highest correspondence to both behavioral and human brain representations, our results indicate that more recent, deeper neural network models are not necessarily preferred over previous, shallower models, at least when exclusively leveraging the penultimate layer of a network. Their correspondences appear to be highly dataset-dependent. Although a pretrained version of AlexNet correlated poorly with representations obtained from behavioral experiments (see Figure 4 (a)), there are datasets where AlexNet showed close correspondence to brain representations (see Figure 5 (a)). Similarly, VGG16 was mostly outperformed by CLIP-RN, but in one out of five datasets it yielded a higher correlation with behavioral representations than CLIP-RN.

Moreover, for each model combination, we compared their penultimate layer representations against each other for the THINGS image dataset (Hebart et al., 2019), since this dataset was both the largest and most diverse across the datasets we used to demonstrate the applicability of THINGSvision. We computed the Pearson correlation between each model pair's flattened lower RDM triangles, resulting in a symmetric correlation matrix (see Figure 6). This is also called second-order RSA. RDMs were created from network activations of both pretrained models (a) and models with random weights (b).

Not surprisingly, object representations from the penultimate layer of VGG16 and VGG19 showed a high Pearson correlation coefficient ( $r = 0.80$ ). What is interesting, however, is that representations from the penultimate layers of ResNet50 and CORnet-S appeared to achieve a similarly high correlation with the VGG models when leveraging pretrained weights (see Figure 6 (a)), but notably less so when using random weights (see Figure 6 (b)).

Representations from AlexNet's penultimate layer correlated less with object representations from the aforementioned models for random compared to pretrained weights. CLIP-RN and CLIP-ViT correlated highly when comparing their pretrained versions, but seem to correlate only marginally when comparing representations obtained by random weights. Somewhat surprisingly, representations pertaining to CORnet-S correlated more strongly with representations from CLIP-ViT and ResNet50 than with representations corresponding to CLIP-RN, of which the latter has a more similar architecture to ResNet50 than CLIP-ViT.

The above results indicate that representations extracted from the CLIP variants encode different information about visual objects than representations pertaining to the other neural network models, especially when leveraging pretrained model parameters. This might be due to their different architectures (Transformer vs. CNN layers), their different optimization objectives (multimodal vs. unimodal), or an interaction of the two. Future studies are encouraged to investigate this representational difference more closely. To reproduce our results or compare object representations extracted from other models and layers against each other, for a List of models and layers a user can perform the following operation

```
clip_list = [n.startswith('clip') for n in model_names]

correlations = vision.compare_models(
    root=root,
    out_path=out_path,
    model_names=model_names,
    module_names=module_names,
    pretrained=True,
    batch_size=batch_size,
    flattenActs=True,
    clip=clip_list,
    save_features=True,
    dissimilarity='correlation',
    correlation='pearson',
)
```

The function returns a correlation matrix in the form of a Pandas dataframe whose rows

and columns correspond to the names of the models in `model_names`. The cell elements are the correlation coefficients for each model combination.

### 3.3 Convolutional blocks

To visualize how representations change across layers for different neural network architectures, we additionally computed RDMs for features extracted from each of the sixteen convolutional blocks in both ResNet50 (He et al., 2016) and the CLIP variant of ResNet50 (Radford et al., 2021) for three datasets used for fMRI recordings of the primate visual system (Cichy et al., 2016, 2014; Mohsenzadeh et al., 2019). A convolutional block is composed of three convolutional layers, each of which is followed by a pooling layer and batch normalization (Ioffe & Szegedy, 2015). For each block, we extracted features at the last batch normalization layer, prior to the rectifier non-linearity. The RDMs in Figure 7 suggest that the more one progresses in the layer hierarchy of ResNet50 and CLIP-RN, the more the representations of the two models differ qualitatively. This could explain the differences between ResNet50 and CLIP-RN when compared to representations extracted from behavioral experiments (see Figure 4), which are considered abstract and, thus, correspond to layers at the top of a model.

## 4 Discussion

Here we introduce **THINGSvision**, a Python toolbox for extracting activations from hidden layers of a wide range of deep neural network models. We designed **THINGSvision** to facilitate research at the intersection of cognitive science, computational neuroscience, and artificial intelligence.

Recently, an API was released (Mehrer, Spoerer, Jones, Kriegeskorte, & Kietzmann, 2021) that enables the extraction of image features from AlexNet and vNet without the requirement to install any library, making it a highly user-friendly contribution to the field. Apart from requiring an installation of Python, **THINGSvision** provides a comparably simple way to extract network activations, yet for a much broader set of DNNs and with a higher degree of flexibility and control over the extraction procedure. **THINGSvision** can easily be integrated with any other computational analysis pipeline performed in Python or Matlab. We additionally allow for a streamlined comparison of visual object representations obtained from various DNNs employing representational similarity analysis.

We demonstrated the usefulness of **THINGSvision** through the application of RSA and the quantification of correspondences between representations extracted from models and human behavior (or brains). **THINGSvision** enabled us to investigate object representations of CLIP (Radford et al., 2021) against representations extracted from other neural network models as well as representations from behavioral experiments and fMRI responses to higher visual cortex.

To understand why Transformer layers and multimodal training objectives help to achieve strong correspondences to behavioral representations (see Figure 4) and lead to both qualitative differences to the original version of ResNet50 at top layers (see Figure 7) and lower Pearson correlation coefficients to other neural network models (see Figure 6), further studies are encouraged to investigate the representations of CLIP and its differences to previous DNN architectures with unimodal objectives. We hope that **THINGSvision** will serve as a useful tool that supports researchers in carrying out such analyses, and we intend to extend the set of models and functionalities that are integral to **THINGSvision** over the coming years as a function of advancements and demands in the field.

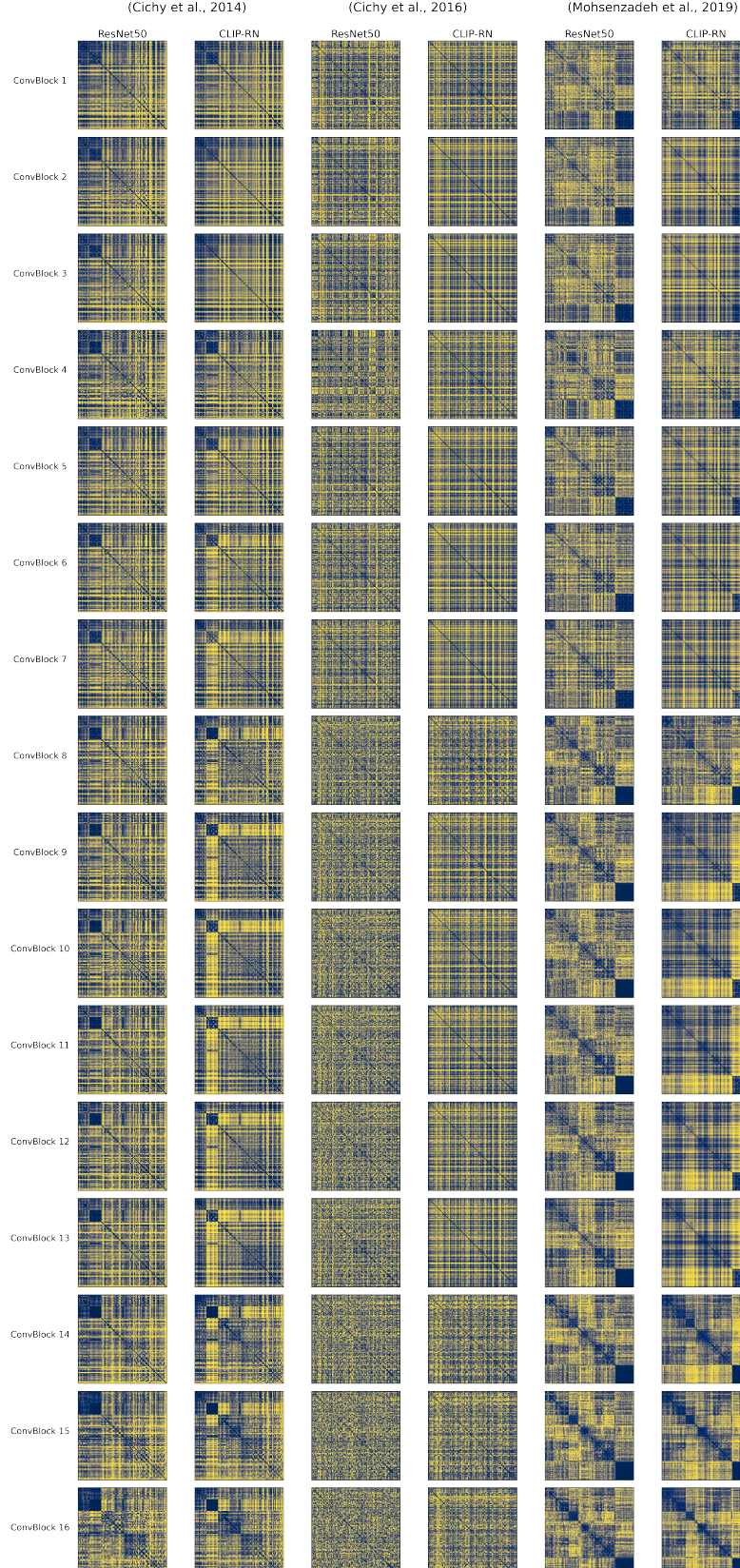


**Figure 7:** RDMs for representations extracted from each of the convolutional blocks in ResNet50 and CLIP-RN. Rows refer to convolutional blocks, enumerated from bottom to top. First two columns: (Cichy et al., 2014). Two columns in the center: (Cichy et al., 2016). Last two columns: (Mohsenzadeh et al., 2019).

## Acknowledgements

The authors would like to thank Katja Seeliger, Oliver Contier and Philipp Kaniuth for useful comments on earlier versions of this paper and for helpful feedback concerning the use of the software.

## Funding Statement

This work was supported by a Max Planck Research Group grant of the Max Planck Society awarded to MNH.

## Competing interests

The authors have no competing interests to declare.

## References

- Arbuckle, S. A., Yokoi, A., Pruszynski, J. A., & Diedrichsen, J. (2019). Stability of representational geometry across a wide range of fmri activity levels. *NeuroImage*, 186, 155-163. DOI: <https://doi.org/10.1016/j.neuroimage.2018.11.002>
- Bankson, B., Hebart, M., Groen, I., & Baker, C. (2018). The temporal evolution of conceptual object representations revealed through models of behavior, semantics and deep neural networks. *NeuroImage*, 178, 172-182. DOI: <https://doi.org/10.1016/j.neuroimage.2018.05.037>
- Battleday, R. M., Peterson, J. C., & Griffiths, T. L. (2019). Capturing human categorization of natural images at scale by combining deep networks and cognitive models. *CoRR*, *abs/1904.12690*.
- Cichy, R. M., Khosla, A., Pantazis, D., Torralba, A., & Oliva, A. (2016). *Comparison of deep neural networks to spatio-temporal cortical dynamics of human visual object recognition reveals hierarchical correspondence* (Vol. 6) (No. 1). Nature Publishing Group.
- Cichy, R. M., Kriegeskorte, N., Jozwik, K. M., van den Bosch, J. J., & Charest, I. (2019). The spatiotemporal neural dynamics underlying perceived similarity for real-world objects. *NeuroImage*, 194, 12-24. DOI: <https://doi.org/10.1016/j.neuroimage.2019.03.031>
- Cichy, R. M., Pantazis, D., & Oliva, A. (2014). Resolving human object recognition in space and time. *Nature neuroscience*, 17(3), 455.
- Deng, J., Dong, W., Socher, R., Li, L., Li, K., & Li, F. (2009). *Imagenet: A large-scale hierarchical image database*. IEEE Computer Society. DOI: 10.1109/CVPR.2009.5206848
- Dosovitskiy, A., Beyer, L., Kolesnikov, A., Weissenborn, D., Zhai, X., Unterthiner, T., ... Houlsby, N. (2020). An image is worth 16x16 words: Transformers for image recognition at scale. *CoRR*, *abs/2010.11929*.
- Esteban, O., Markiewicz, C. J., Blair, R. W., Moodie, C. A., Isik, A. I., Erramuzpe, A., ... Gorgolewski, K. J. (2018, December). fMRIprep: a robust preprocessing pipeline for functional MRI. *Nature Methods*, 16(1), 111–116. DOI: 10.1038/s41592-018-0235-4
- Grootswagers, T., & Robinson, A. K. (2021). *Overfitting the literature to one set of stimuli and data*.
- Güçlü, U., & van Gerven, M. A. J. (2014, august). Unsupervised feature learning improves prediction of human brain activity in response to natural images. *PLoS Computational Biology*, 10(8), e1003724. DOI: 10.1371/journal.pcbi.1003724
- Harris, C. R., Millman, K. J., van der Walt, S., Gommers, R., Virtanen, P., Cournapeau, D., ... Oliphant, T. E. (2020). Array programming with NumPy. *Nature*, 585(7825), 357–362. DOI: 10.1038/s41586-020-2649-2
- He, K., Zhang, X., Ren, S., & Sun, J. (2016). Deep residual learning for image recognition. In *2016 IEEE conference on computer vision and pattern recognition, CVPR 2016, las vegas, nv, usa, june 27-30, 2016* (pp. 770–778). IEEE Computer Society. DOI: 10.1109/CVPR.2016.90
- Hebart, M. N., Dickter, A. H., Kidder, A., Kwok, W. Y., Corriveau, A., Van Wicklin, C., & Baker, C. I. (2019). *Things: A database of 1,854 object concepts and more than 26,000 naturalistic object images* (Vol. 14) (No. 10). Public Library of Science San Francisco, CA USA.
- Hebart, M. N., Zheng, C. Y., Pereira, F., & Baker, C. I. (2020, October). Revealing the multidimensional mental representations of natural objects underlying human similarity

- judgements. *Nature Human Behaviour*, 4(11), 1173–1185. DOI: 10.1038/s41562-020-00951-3
- Ioffe, S., & Szegedy, C. (2015). Batch normalization: Accelerating deep network training by reducing internal covariate shift. In F. R. Bach & D. M. Blei (Eds.), *Proceedings of the 32nd international conference on machine learning, ICML 2015, lille, france, 6-11 july 2015* (Vol. 37, pp. 448–456). JMLR.org.
- Jozwik, K. M., Kriegeskorte, N., Cichy, R. M., & Mur, M. (2018). Deep convolutional neural networks, features, and categories perform similarly at explaining primate high-level visual representations. In *2018 conference on cognitive computational neuroscience. Cognitive Computational Neuroscience*. DOI: 10.32470/ccn.2018.1232-0
- Kaniuth, P., & Hebart, M. N. (2020, October). Tuned representational similarity analysis: Improving the fit between computational models of vision and brain data. *Journal of Vision*, 20(11), 1076. DOI: 10.1167/jov.20.11.1076
- Khaligh-Razavi, S.-M., & Kriegeskorte, N. (2014, November). Deep supervised, but not unsupervised, models may explain IT cortical representation. *PLoS Computational Biology*, 10(11), e1003915. DOI: 10.1371/journal.pcbi.1003915
- Kietzmann, T. C., McClure, P., & Kriegeskorte, N. (2018). Deep neural networks in computational neuroscience. *BioRxiv*(133504), 1-28.
- King, M. L., Groen, I. I., Steel, A., Kravitz, D. J., & Baker, C. I. (2019). Similarity judgments and cortical visual responses reflect different properties of object and scene categories in naturalistic images. *NeuroImage*, 197, 368-382. DOI: <https://doi.org/10.1016/j.neuroimage.2019.04.079>
- Kriegeskorte, N. (2015). Deep neural networks: A new framework for modeling biological vision and brain information processing. *Annual Review of Vision Science*, 1(1), 417-446. (PMID: 28532370) DOI: 10.1146/annurev-vision-082114-035447
- Kriegeskorte, N., Mur, M., & Bandettini, P. A. (2008). Representational similarity analysis-connecting the branches of systems neuroscience. *Frontiers in Systems Neuroscience*, 2, 1-28.
- Kriegeskorte, N., Mur, M., Ruff, D. A., Kiani, R., Bodurka, J., Esteky, H., ... Bandettini, P. A. (2008). Matching categorical object representations in inferior temporal cortex of man and monkey. *Neuron*, 60(6), 1126–1141.
- Krizhevsky, A., Sutskever, I., & Hinton, G. E. (2012). Imagenet classification with deep convolutional neural networks. In F. Pereira, C. J. C. Burges, L. Bottou, & K. Q. Weinberger (Eds.), *Advances in neural information processing systems* (Vol. 25, pp. 1097–1105). Curran Associates, Inc.
- Kubilius, J., Schrimpf, M., Hong, H., Majaj, N. J., Rajalingham, R., Issa, E. B., ... DiCarlo, J. J. (2019). Brain-like object recognition with high-performing shallow recurrent anns. In H. M. Wallach, H. Larochelle, A. Beygelzimer, F. d'Alché-Buc, E. B. Fox, & R. Garnett (Eds.), *Advances in neural information processing systems 32: Annual conference on neural information processing systems 2019, neurips 2019, december 8-14, 2019, vancouver, bc, canada* (pp. 12785–12796).
- Kubilius, J., Schrimpf, M., Nayebi, A., Bear, D., Yamins, D. L., & DiCarlo, J. J. (2018). Cornet: Modeling the neural mechanisms of core object recognition. *BioRxiv*, 408385.
- LeCun, Y., Bengio, Y., & Hinton, G. (2015). Deep learning. *nature*, 521(7553), 436–444.
- Mehrer, J., Spoerer, C. J., Jones, E. C., Kriegeskorte, N., & Kietzmann, T. C. (2021). An ecologically motivated image dataset for deep learning yields better models of human vision. *Proceedings of the National Academy of Sciences*, 118(8).

DOI: 10.1073/pnas.2011417118

- Mohsenzadeh, Y., Mullin, C., Lahner, B., Cichy, R. M., & Oliva, A. (2019). *Reliability and generalizability of similarity-based fusion of meg and fmri data in human ventral and dorsal visual streams* (Vol. 3) (No. 1). Multidisciplinary Digital Publishing Institute.
- Mur, M., Meys, M., Bodurka, J., Goebel, R., Bandettini, P., & Kriegeskorte, N. (2013). *Human object-similarity judgments reflect and transcend the primate-it object representation* (Vol. 4). DOI: 10.3389/fpsyg.2013.00128
- Nili, H., Wingfield, C., Walther, A., Su, L., Marslen-Wilson, W., & Kriegeskorte, N. (2014, April). A toolbox for representational similarity analysis. *PLoS Computational Biology*, 10(4), e1003553. DOI: 10.1371/journal.pcbi.1003553
- Paszke, A., Gross, S., Massa, F., Lerer, A., Bradbury, J., Chanan, G., ... Chintala, S. (2019). Pytorch: An imperative style, high-performance deep learning library. In H. M. Wallach, H. Larochelle, A. Beygelzimer, F. d'Alché-Buc, E. B. Fox, & R. Garnett (Eds.), *Advances in neural information processing systems 32: Annual conference on neural information processing systems 2019, neurips 2019, december 8-14, 2019, vancouver, bc, canada* (pp. 8024–8035).
- Peng, R. D. (2011). Reproducible research in computational science. *Science*, 334(6060), 1226–1227. DOI: 10.1126/science.1213847
- Peterson, J. C., Abbott, J. T., & Griffiths, T. L. (2018). Evaluating (and improving) the correspondence between deep neural networks and human representations. *Cognitive science*, 42(8), 2648–2669.
- Radford, A., Kim, J. W., Hallacy, C., Ramesh, A., Goh, G., Agarwal, S., ... others (2021). Learning transferable visual models from natural language supervision. *arXiv*.
- Rush, A. (2018, July). The annotated transformer. In *Proceedings of workshop for NLP open source software (NLP-OSS)* (pp. 52–60). Melbourne, Australia: Association for Computational Linguistics. DOI: 10.18653/v1/W18-2509
- Russakovsky, O., Deng, J., Su, H., Krause, J., Satheesh, S., Ma, S., ... Li, F. (2015). Imagenet large scale visual recognition challenge. *Int. J. Comput. Vis.*, 115(3), 211–252. DOI: 10.1007/s11263-015-0816-y
- Schrimpf, M., Kubilius, J., Hong, H., Majaj, N. J., Rajalingham, R., Issa, E. B., ... DiCarlo, J. J. (2018). Brain-score: Which artificial neural network for object recognition is most brain-like? *bioRxiv preprint*.
- Schrimpf, M., Kubilius, J., Lee, M. J., Murty, N. A. R., Ajemian, R., & DiCarlo, J. J. (2020). Integrative benchmarking to advance neurally mechanistic models of human intelligence. *Neuron*.
- Simonyan, K., & Zisserman, A. (2015). Very deep convolutional networks for large-scale image recognition. In Y. Bengio & Y. LeCun (Eds.), *3rd international conference on learning representations, ICLR 2015, san diego, ca, usa, may 7-9, 2015, conference track proceedings*.
- Storrs, K. R., Khaligh-Razavi, S.-M., & Kriegeskorte, N. (2020). Noise ceiling on the crossvalidated performance of reweighted models of representational dissimilarity: Addendum to khaligh-razavi & kriegeskorte (2014). *bioRxiv*. DOI: 10.1101/2020.03.23.003046
- Van Lissa, C. J., Brandmaier, A. M., Brinkman, L., Lamprecht, A.-L., Peikert, A., Struiksma, M., & Vreede, B. (2020). Worcs: A workflow for open reproducible code in science. *PsyArXiv*.
- Vaswani, A., Shazeer, N., Parmar, N., Uszkoreit, J., Jones, L., Gomez, A. N., ... Polosukhin, I. (2017). Attention is all you need. In I. Guyon et al. (Eds.), *Advances in*

*neural information processing systems 30: Annual conference on neural information processing systems 2017, december 4-9, 2017, long beach, ca, USA* (pp. 5998–6008).

Wang, A., Pruksachatkun, Y., Nangia, N., Singh, A., Michael, J., Hill, F., ... Bowman, S. R.

(2019). Superglue: A stickier benchmark for general-purpose language understanding systems. In H. M. Wallach, H. Larochelle, A. Beygelzimer, F. d'Alché-Buc, E. B. Fox, & R. Garnett (Eds.), *Advances in neural information processing systems 32: Annual conference on neural information processing systems 2019, neurips 2019, december 8-14, 2019, vancouver, bc, canada* (pp. 3261–3275).

Wang, A., Singh, A., Michael, J., Hill, F., Levy, O., & Bowman, S. R. (2018). GLUE:

A multi-task benchmark and analysis platform for natural language understanding.

In T. Linzen, G. Chrupala, & A. Alishahi (Eds.), *Proceedings of the workshop: Analyzing and interpreting neural networks for nlp, blackboxnlp@emnlp 2018, brussels, belgium, november 1, 2018* (pp. 353–355). Association for Computational Linguistics.

DOI: 10.18653/v1/w18-5446

Yamins, D. L. K., Hong, H., Cadieu, C. F., Solomon, E. A., Seibert, D., & DiCarlo, J. J.

(2014). Performance-optimized hierarchical models predict neural responses in higher visual cortex. *Proceedings of the National Academy of Sciences*, 111(23), 8619–8624.

DOI: 10.1073/pnas.1403112111

# A Appendix

## A.1 Basic function call flow

THINGSvision equips users with different possibilities on how to select modules and enables them to choose whether or not to compute or visualize RDMs for the extracted features. Figure 8 displays the basic function calls a user has to make to extract features and compute or visualize and save RDMs, in their recommended order. There are, however, other functionalities whose usefulness we demonstrated throughout the paper but did not include in the flowchart since they are not part of the basic THINGSvision feature extraction flow.

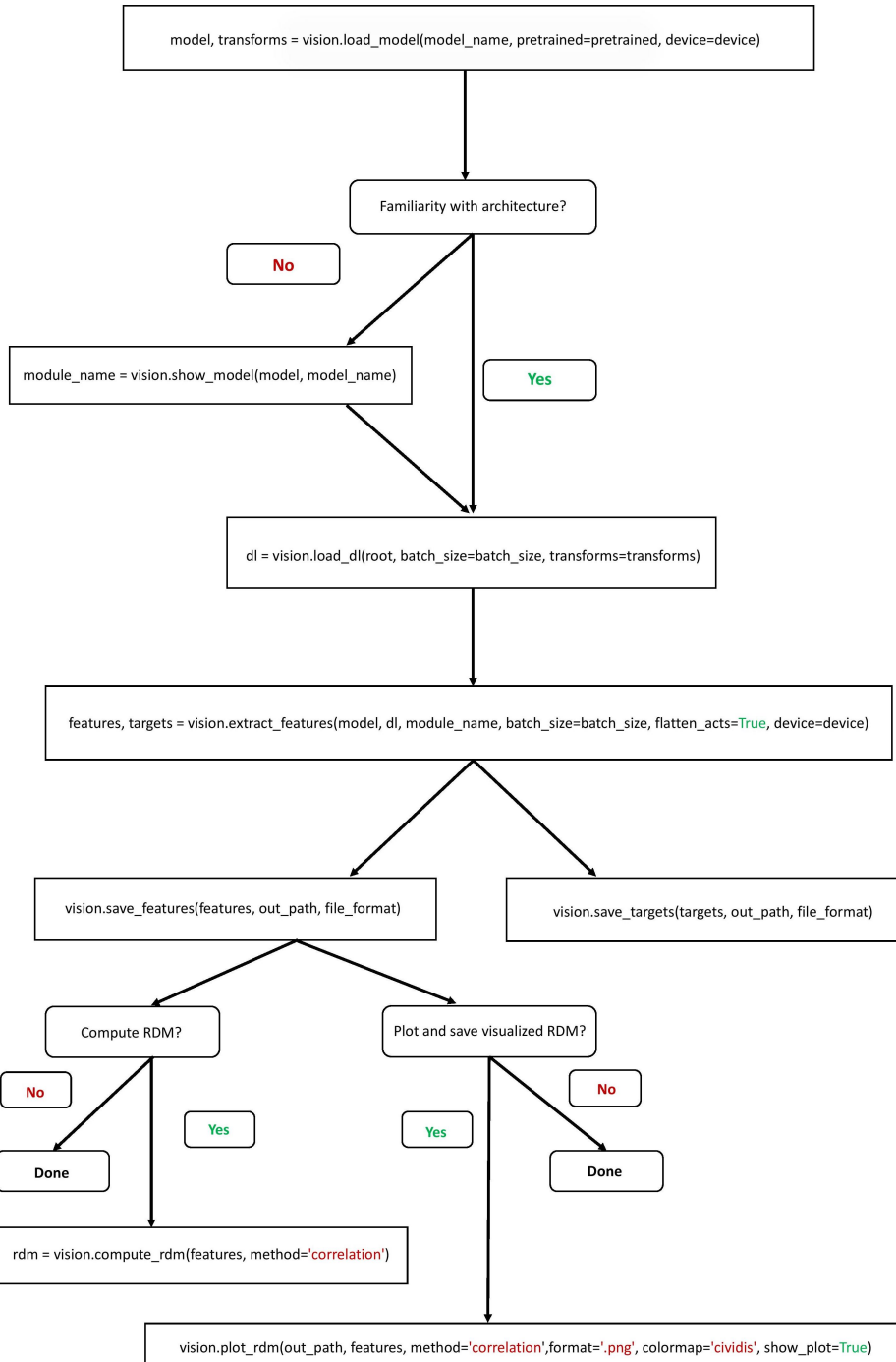


**Figure 8:** THINGSvision’s function call flowchart.